Interaction of the gp120 V1V2 loop with a neighboring gp120 unit shields the HIV envelope trimer against cross-neutralizing antibodies

Peter Rusert,[1] Anders Krarup,[1] Carsten Magnus,[4] Oliver F. Brandenberg,[1,2] Jacqueline Weber,[1] Anna-Katharina Ehlert,[1] Roland R. Regoes,[4] Huldrych F. Günthard,[3] and Alexandra Trkola[1]

[1]Institute of Medical Virology; [2]PhD Program in Microbiology and Immunology; and [3]Division of Infectious Diseases and Hospital Epidemiology, University Hospital Zurich; University of Zurich, 8006 Zurich, Switzerland
[4]Institute of Integrative Biology, Swiss Federal Institute of Technology Zurich, 8092 Zurich, Switzerland

The HIV-1 envelope trimer adopts a quaternary conformation that effectively shields neutralization-sensitive domains and thus represents a major obstacle for natural and vaccine-elicited antibody responses. By using a structure–function analysis based on a specifically devised mathematical model, we demonstrate in this study that protection from neutralization is enforced by intersubunit contact between the variable loops 1 and 2 (V1V2) and domains of neighboring gp120 subunits in the trimer encompassing the V3 loop. Our data are consistent with an interaction of the V1V2 and V3 loop at the spike apex as proposed by cryoelectron tomography experiments. By defining the orientation of the V1V2 loop within the trimer toward the neighboring gp120 subunit's V3 loop, our data close an important gap in the understanding of the architecture of the trimeric spike. Knowledge on how the V1V2 barrier functions in the context of the trimer to mask conserved epitopes on gp120 may aid future vaccine design.

CORRESPONDENCE
Alexandra Trkola:
trkola.alexandra@virology.uzh.ch

Abbreviations used: CD4bs, CD4 binding site; CD4i, CD4 induced; cryo-ET, cryo-electron tomography; Env, envelope; MFI, mean fluorescent intensity.

A large body of information on the HIV-1 gp120 envelope (Env) glycoprotein variable loop domains 1 and 2 (V1 and V2) has accumulated over the years. Neither domain is absolutely necessary for the virus. Deletion of either or both loops has been shown to be tolerable in the context of specific virus strains and can yield replication-competent viruses (Wyatt et al., 1993, 1995; Cao et al., 1997; Stamatatos and Cheng-Mayer, 1998; Stamatatos et al., 1998; Saunders et al., 2005; Laakso et al., 2007; Bontjer et al., 2009). Although length polymorphism and the changing glycosylation pattern of the V1V2 domain during disease progression have long been appreciated (Palmer et al., 1996; Chackerian et al., 1997; Fox et al., 1997; Shioda et al., 1997; Masciotra et al., 2002; Kitrinos et al., 2003; Chohan et al., 2005; Sagar et al., 2006; Harrington et al., 2007), uncertainty prevails to date on which selective forces drive V1V2 evolution. To what extent virus quasispecies with decreased V1V2 length and glycosylation are preferentially transmitted or have a selective advantage in early infection is not fully understood (Derdeyn et al., 2004; Ritola et al., 2004; Frost et al., 2005; Liu et al., 2008b) and neither are the precise roles of the V1V2 domain in viral attachment and cell–cell spread (Pastore et al., 2006; Sagar et al., 2006; Arthos et al., 2008; Cicala et al., 2009). However, the profound influence of the V1V2 domain on the virus' susceptibility to neutralization is well documented as deletions and mutations within the V1 and V2 loop (especially those that affect glycosylation sites) were found to increase sensitivity to neutralizing antibodies (Cao et al., 1997; Chackerian et al., 1997; Fox et al., 1997; Morikita et al., 1997; Stamatatos and Cheng-Mayer, 1998; Ly and Stamatatos, 2000; Losman et al., 2001; Johnson et al., 2003; Cole et al., 2004; Pinter et al., 2004;

A. Krarup, C. Magnus, and O.F. Brandenberg contributed equally to this paper.

The Rockefeller University Press $30.00
J. Exp. Med. Vol. 208 No. 7 1419-1433
www.jem.org/cgi/doi/10.1084/jem.20110196

The Journal of Experimental Medicine

Pugach et al., 2004; Krachmarov et al., 2005, 2006; Saunders et al., 2005; Sagar et al., 2006; Shibata et al., 2007; Ching et al., 2008). Collectively, these studies suggest that the V1V2 loop can both function as a direct target for neutralizing antibodies elicited in vivo and shield distant neutralization-sensitive domains on the viral Env such as the V3 loop, CD4-induced (CD4i) epitopes, and the CD4 binding site (CD4bs; Sanders et al., 2000; Saunders et al., 2005; Laakso et al., 2007; Bontjer et al., 2009). Of note, the recent discovery of highly potent neutralizing antibodies that recognize quaternary epitopes encompassing the V2 loop have highlighted once more the potential impact of the V1V2-directed immune response (Gorny et al., 2005; Walker et al., 2009). Importantly, on a population level, the past decades of continuous neutralizing antibody–driven evolution of the V1V2 during the pandemic have been suggested to have led to the acquisition of longer, more glycosylated V1V2 domains that render current HIV isolates increasingly neutralization resistant (Bunnik et al., 2010). Understanding how the V1V2 domain steers neutralization sensitivity is thus of pivotal importance to allow vaccine-induced antibody responses to be tailored to counteract its effect.

How V1V2 shielding is provided for in the context of the native Env spike necessitates the definition of the three-dimensional geometry of the spike and in particular the intersubunit contact areas. Although over the years crystal structure analysis of the HIV Env has unraveled structural features of ligand-bound and unliganded, monomeric gp120 variants at great depth and at high resolution (Kwong et al., 1998, 2000, 2002; Chen et al., 2005; Zhou et al., 2007; Chen et al., 2009; Diskin et al., 2010; Finzi et al., 2010; Kong et al., 2010; Pancera et al., 2010; Xiang et al., 2010), structural information on the variable loops within HIV-1 gp120 is still scarce (Huang et al., 2005) and in the case of the V1V2 loop missing. Earlier studies have proposed a potential intersubunit contact between the V1V2 and V3 loop (Kwong et al., 2000; Chen et al., 2005). Thus, V1V2 domains could potentially protect the V3 loop on neighboring (adjacent) gp120 subunits within the Env trimer. In recent years, cryoelectron tomography (cryo-ET) studies have brought important insights on the three-dimensional organization of the Env spike (Zanetti et al., 2006; Zhu et al., 2006; Liu et al., 2008a; White et al., 2010; Wu et al., 2010). Although cryo-ET yet lacks the resolution to precisely and unambiguously define intersubunit contact areas within the native spike, data available to date suggest that heterotypic loop interactions of the V1V2 and V3 loops may indeed occur in the apex of the spike (Liu et al., 2008a; White et al., 2010; Wu et al., 2010). These findings further support the notion that V1V2 shielding may indeed involve an inter- or intra-subunit interaction with the V3 loop.

RESULTS

High titered cross-reactive plasma antibody response is efficiently shielded by the V1V2 loop

Past investigations on the influence of the V1V2 loop on steering neutralization activity have been restricted to few, mostly highly neutralization-sensitive isolates (HxB2, LAI, SF162, R3A, and YU-2; Wyatt et al., 1993, 1995; Cao et al., 1997; Stamatatos and Cheng-Mayer, 1998; Stamatatos et al., 1998; Sullivan et al., 1998; Saunders et al., 2005; Laakso et al., 2007; Bontjer et al., 2009) and thus left a definite verdict on the potency of the V1V2 loop shielding effect against primary viruses pending. In this study, we generated a panel of six infection-competent V1V2 loop–deleted Env's of tier 1 (NL4-3 and SF162), tier 2 (JR-FL*, RHPA, and REJO), and tier 3 (ZA110.c10.14) subtype B isolates by inserting the linker sequence Asp-Ala-Gly (DAG) as described previously (Fig. S1 A and Table S1; Bontjer et al., 2009). WT and matching V1V2-deleted viruses were then compared for sensitivity to neutralization by plasma samples from 83 individuals with chronic HIV infection from different genetic subtypes (Fig. 1 A and Tables S3 and S4). In the absence of the shielding effect of the V1V2, potent cross-neutralization activity was detected in all probed patient plasma samples with some neutralization titers exceeding those of WT viruses by more than four orders of magnitude.

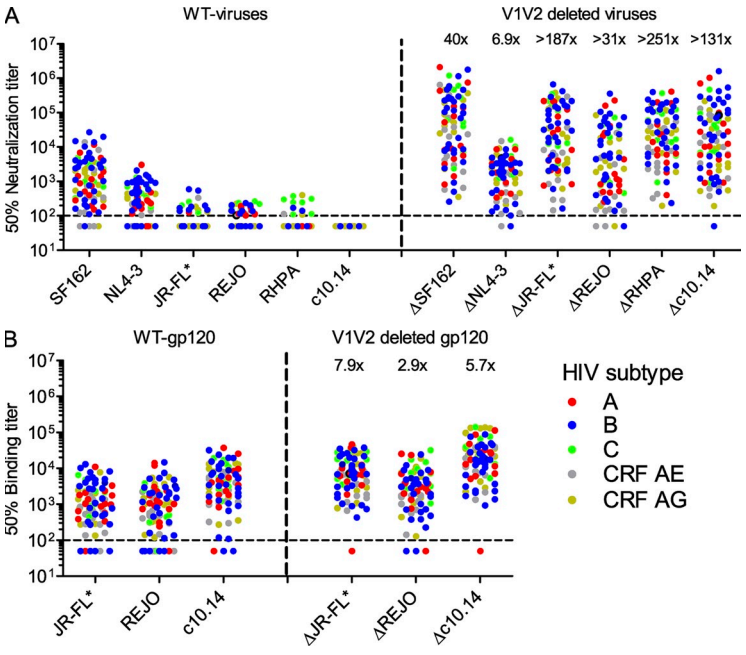

Figure 1. Effect of V1V2 shielding on plasma antibody neutralization. (A) Cross-neutralization activity (50%) was investigated in 83 plasma samples from individuals chronically infected with divergent HIV subtypes (indicated by differentially colored data points). Neutralization activity against six WT viruses (left) and corresponding V1V2-deleted mutants (right) are shown. (B) Efficacy of patient plasma antibody binding to WT or V1V2-deleted gp120 (50%) was estimated by ELISA. (A and B) Data are derived from two to three independent experiments. The dashed lines correspond to the lowest plasma dilution tested (1:100). Fold increases (x) in median neutralization and binding titers of V1V2-deleted Env's compared with the corresponding WT Env are indicated above each panel.

Of note, the neutralization-sensitive, CXCR4-using, T cell line–adapted virus NL4-3 portrayed the least increase (6.9-fold) in susceptibility to neutralization upon removal of its V1V2 domain. Although absolute neutralization titers against V1V2-deleted SF162 matched those of the other four R5 viruses, the fold increase in neutralization sensitivity of SF162 upon V1V2 deletion was also lower (40-fold) as SF162 WT was efficiently inhibited by the patient plasma samples. Plasma neutralization titers against the V1V2-deleted isolates were tightly correlated (Table S5), suggesting that common antibody types were elicited across subtypes that target conserved, highly neutralization-sensitive epitopes usually shielded by the V1V2 domain. Interestingly, although gp120 binding and neutralization efficacies correlated (Table S5), only modest increases in binding efficacy of V1V2-deleted gp120 were evident (Fig. 1 B and Table S4). The latter strongly supports the notion that the V1V2 domain exerts its full shielding effect only in the context of the intact viral spike and not on monomeric gp120. Nevertheless, a comparison of binding and neutralizing antibodies in the context of polyclonal plasma has to be interpreted with caution as neutralizing antibodies may quantitatively represent only a small fraction of the overall binding antibodies in patient sera.

Delineating neutralizing antibody epitopes shielded by the V1V2 domain

To understand which neutralizing antibody epitopes are protected by the V1V2, we probed the shielding effect of the V1V2 domain for mAbs targeting diverse epitopes within gp120 and gp41 by comparing their ability to neutralize WT and V1V2-deleted viruses or to bind to respective monomeric gp120 proteins (Fig. 2 and Tables S1 and S2). Of all the epitope specificities probed, V1V2 shielding had the most dramatic effect on V3 loop antibodies with up to 240,000-fold higher neutralization titers against a V1V2-deleted virus. Masking by the V1V2 of both V3 loop and CD4bs was dependent on the trimeric state of the Env, as binding efficacies to WT and mutant gp120 proteins were essentially identical (Fig. 2). gp41-specific reagents were included as controls as direct V1V2 shielding of these epitopes is unlikely. Accordingly, only modest effects on their inhibitory capacity were evident, confirming that V1V2 deletion did not inflict gross changes in entry efficacy or trimer stability that would impair further analysis using these mutants. Neutralization potency of CD4i-specific mAbs increased in comparison only moderately, and no or only modest effects were evident for the glycan-specific mAb 2G12. Interestingly, CD4bs-directed inhibitors were differentially affected by V1V2 shielding. Depending on the isolate probed, CD4bs mAbs b12 and VRC01 either neutralized with identical or decreased activity in the absence of the V1V2, highlighting that these antibodies have found a unique way to bypass or even take advantage of the V1V2 domain. All other CD4bs agents probed (tetrameric CD4-IgG2, mAbs

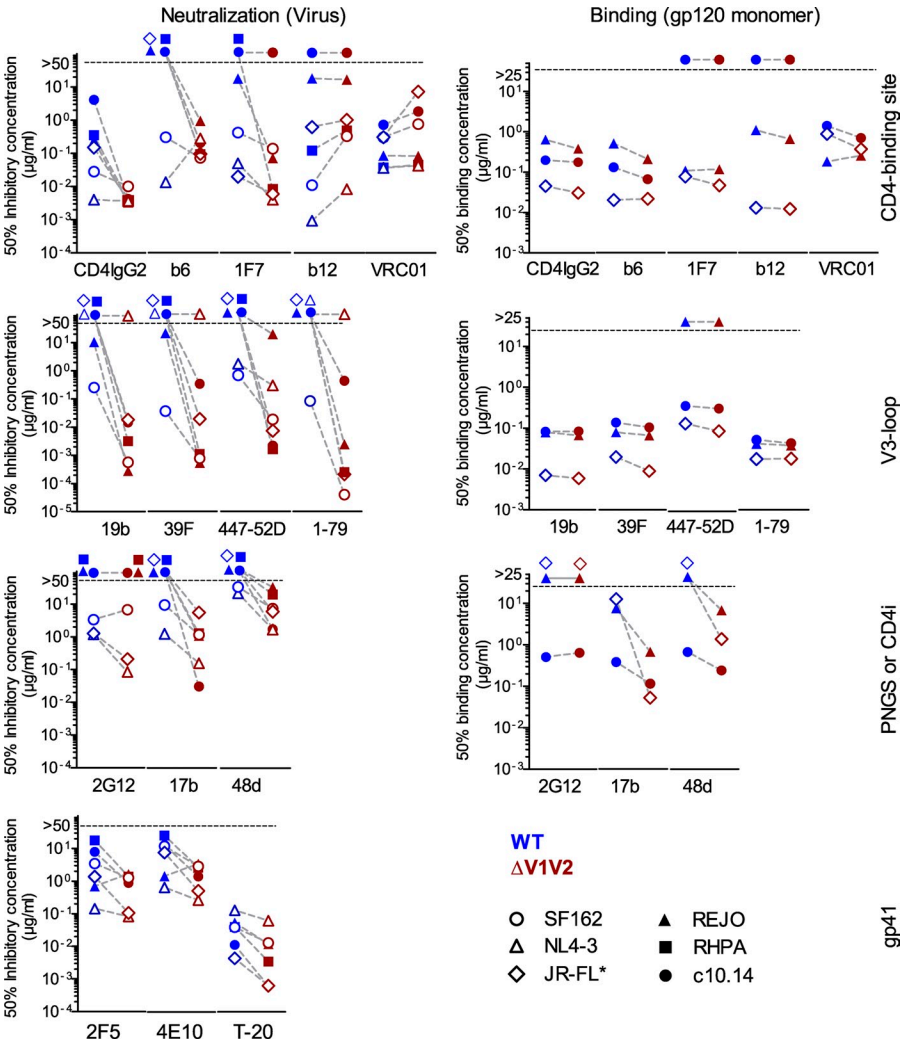

Figure 2. The V1V2 shapes inhibitory activity of neutralizing antibodies. The 50% inhibitory (left) and 50% gp120 binding concentrations (right) of HIV Env–specific antibodies and inhibitors (listed on the x axis) against WT and the corresponding V1V2-deleted Env viruses (SF162, NL4-3, JR-FL*, REJO, RHPA, and c10.14) are shown. The dashed lines represent the highest concentration tested (50 µg/ml and 25 µg/ml for neutralization and binding assays, respectively). Targets of antibodies and inhibitors are shown on the right. Data are derived from two to three independent experiments. PNGS, potential N-linked glycosylation site.

b6 and 1F7) greatly improved neutralization activity upon V1V2 deletion for those isolates that were not inhibited as efficiently as WT, indicating a substantial influence of the V1V2 domain on access to their respective epitopes. In sum, our data suggest that the ability of b12 and VRC01 to bypass or take advantage of the V1V2 in binding to the trimeric spike likely accounts for their broad and potent activity. We next compared binding of mAbs to monomeric WT and V1V2-deleted gp120 proteins to obtain initial insight whether the V1V2 masking of their respective epitopes occurs in the context of the trimer or monomer (Fig. 2). Notably, only CD4i mAbs improved their binding capacity to the V1V2-deleted gp120 proteins, suggesting that in the absence of CD4 triggering, access to CD4i epitopes on monomeric gp120 is restricted by the V1V2 loop. Alternatively, the intrinsic equilibrium between gp120 conformations that do not present the CD4i domain versus such that do may favorably be shifted toward the latter in the absence of the V1V2 loop.

Accessibility to all other probed epitopes on monomeric gp120 was not influenced by the V1V2 loop, and binding of mAbs to WT and V1V2-deleted monomeric gp120 occurred at comparable levels. Of particular note, this was also true for inhibitors targeting the CD4bs and the V3 loop, which were neutralized with a several magnitude higher potency in the absence of the V1V2 loop. Thus, effective shielding of these domains by the V1V2 loop entirely depends on the organization of the Env proteins in the native, trimeric spike.

The V1V2 loop counteracts a potent R5 V3 loop–specific cross-neutralization activity commonly elicited in vivo

Our data highlight a remarkably potent effect of the V1V2 shielding on V3 loop–specific mAbs that was comparable in magnitude with the increase in neutralization of V1V2-deleted viruses by patient plasma (Fig. 1 A). It was thus prudent to probe whether V3 loop–specific antibodies are the dominant category of cross-neutralizing antibodies elicited in HIV infection that are counteracted by the V1V2 loop. To this end, we compared the neutralization activity of subtype B plasma samples against V1V2-deleted viruses in the presence or absence of competing peptide encompassing the tip of their cognate V3 loop (Fig. 3, A and B; and Table S1). The outcome of these experiments was astonishingly clear. Cross-neutralization activity against the V1V2-deleted R5 viruses ΔSF162, ΔJR-FL*, and Δ10.14 diminished by several orders of magnitude in the presence of the competing V3 loop peptide in the majority of the probed plasma samples. Thus, V3 loop–reactive antibodies are commonly elicited in HIV infection and are counteracted by the V1V2 domain. Of note, a >90% proportion of the plasma neutralization activity was caused by V3 loop–directed antibodies in 26, 24, and 14 of the 28 probed plasma samples for ΔSF162, ΔJR-FL*, and Δ10.14, respectively (Fig. 3 C). In sharp contrast to the R5 isolates, the NL4-3 V3 loop peptide in large failed to outcompete NL4-3–directed cross-neutralizing plasma activity. Neutralization of NL4-3ΔV1V2 virus in the absence of V3 loop

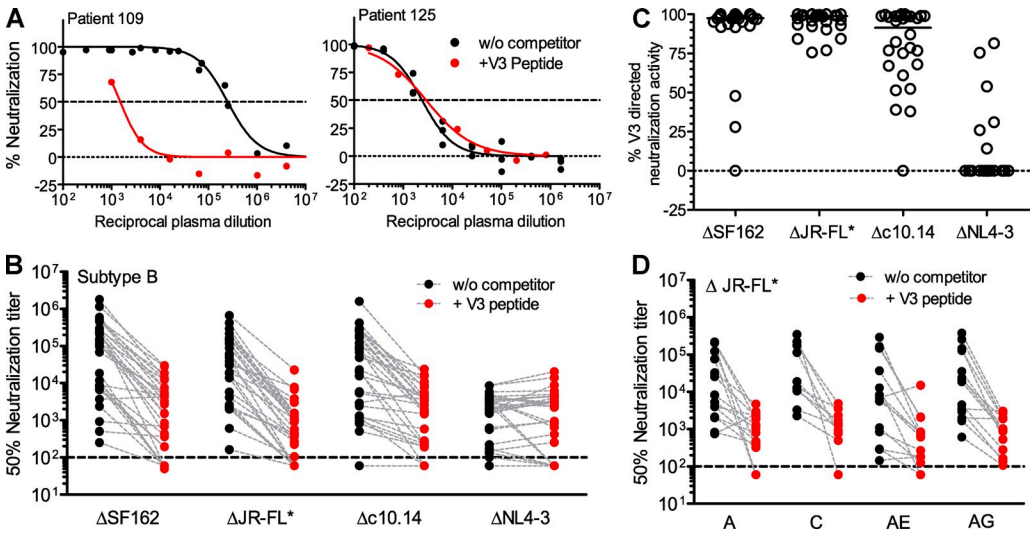

Figure 3. Linear V3 loop peptides compete off V1V2-shielded plasma neutralization activity. Quantification of the contribution of V3 loop antibodies to plasma neutralization by the addition of V3 loop peptides to compete off V3 loop–reactive antibodies. (A) Inhibition profiles of JR-FL* by plasma from two individuals with chronic subtype B infection in the presence (red) or absence (black) of a peptide spanning the tip of the JR-FL V3 loop (Table S1). Representative inhibition profiles from two independent experiments for an individual with a high (patient 109) and an individual with no (patient 125) measurable V3 loop–directed activity in plasma are shown. The dotted line denotes 0% neutralization, and the dashed line denotes 50% neutralization. (B) Analysis of V3 loop antibody contribution to V1V2-deleted virus neutralization in 28 plasma samples derived from chronic subtype B infection. 50% neutralization titers in the presence (red) or absence (black) of the corresponding V3 loop peptide are shown. (C) The fraction of V3 loop–reactive neutralizing antibodies in patient plasma as determined in B is depicted. The dotted line denotes 0% neutralization, and horizontal bars denote medians. (D) Quantification of neutralizing antibodies in patient plasma from individuals infected with non-B subtypes that cross-react with the V3 loop of JR-FL. (B and D) Dashed lines indicate lowest plasma dilution probed (1:100). (B–D) Data are derived from two to three independent experiments. For details on statistical analysis, see Materials and methods.

competition was significantly lower compared with all other probed ΔV1V2 viruses (one-way analysis of variance post-test, Tukey's multiple comparison). However, the fraction of non-V3 loop–reactive antibodies against NL4-3 was comparable with those of the other probed viruses (no significant difference, same test), underlining the fact that V3 loop antibodies do not (or only marginally) contribute to NL4-3 cross-neutralization activity commonly elicited in vivo. The latter likely also accounts for the comparatively low plasma cross-neutralization activity against V1V2-deleted NL4-3 (Fig. 1 A). Whether this reflects a lack of cross-reactivity with specifically the V3 loop of NL4-3 or whether X4 V3 loop–reactive antibodies are generally less frequently elicited in vivo needs to be determined. Humoral immune responses that cross-react with subtype B/R5 V3 loops are commonly elicited in infections of other subtype as JR-FL V3 loop–specific peptide potently competed off JR-FL* cross-neutralizing antibodies in subtypes A, C, AE, and AG plasma (Fig. 3 D). Of note, we found that plasma neutralization activity against WT SF162 is in part mediated by V3 loop–specific antibodies (Fig. S1, B and C). Yet, loss of V1V2 shielding increases V3 loop mAb sensitivity of SF162 substantially (Fig. 3), indicating that V1V2 shielding is, albeit at a lower level, also effective in the context of tier 1 isolates.

The V1V2 loop shields neutralization-sensitive domains on neighboring gp120 units

Unraveling the molecular basis of the shielding effect conferred by the V1V2 loop in the context of the Env spike would provide much needed knowledge on the loop interaction within trimers and overall quaternary trimer architecture not yet available from crystal structure and cryoelectron microscopy analysis. In principle, two mechanisms can be envisaged and have been suggested (Kwong et al., 2000; Chen et al., 2005; Zhu et al., 2006; Liu et al., 2008a; White et al., 2010; Wu et al., 2010): the V1V2 domain can either protect domains in the gp120 subunit it originates from (intrasubunit, self protection) or alternatively act by shielding domains in an adjacent gp120 unit within the trimeric spike (intersubunit, neighboring protection; Fig. 4). Self protection by the V1V2 loops would thereby depend on a substantially altered conformation of the gp120 subunit in the context of the monomer as opposed to the trimer, as only the latter is protected from neutralization by the V1V2 loop (Figs. 1, 2, and 4).

In this study, we devised a mathematical model and an experimental strategy that allows us to distinguish between neighboring and self protection modes of the V1V2 domain. Our chief interest was to define how the V1V2 creates protection for the V3 loop. The basic principle of our approach is to probe the V1V2 shielding effect on the V3 loop in the context of heterogenous Env trimers that are composed of two different types of Env proteins (Fig. 5 A). One WT Env protein (sensitive, harboring V1V2) contains the epitope of the neutralizing V3 loop antibodies 19b and 1-79. The other Env does not contain the epitope for these V3 loop mAbs and was in addition V1V2 deleted (resistant, ΔV1V2). By cotransfecting altering ratios of the two Env-expressing plasmids, cell populations with varying compositions of Env trimers can be generated that consequently differ in the fraction of Env proteins sensitive to V3 loop mAb binding. Depending on whether self or neighboring protection occurs, distinct binding scenarios will be observed (Fig. 5 A).

To differentiate between the two alternative protection scenarios, we devised a mathematical model that predicts the mean number of antibodies bound to a trimer as a function of the fraction of Env proteins carrying the V3 loop mAb–sensitive epitope (Fig. 5 B). Because of the random nature of trimer formation, spikes that contain zero, one, two, or three mAb-sensitive epitopes will form. However, binding of mAb to sensitive V3 loops will only occur on heterotrimers where V1V2 shielding is not effective and will thus depend on whether V1V2 mediates neighboring or self protection (Fig. 5 A). Accordingly, our mathematical model predicts distinct V3 loop mAb–binding patterns in cell populations expressing different compositions of heterotrimers (Fig. 5 B). If the V1V2 loop masks the V3 loop mAb–binding site of the Env protein it originates from, no mAb binding should be observed (Fig. 5 B, green line). In contrast, if the V1V2 loop masks an antibody-binding site of a neighboring Env protein, binding to several trimer configurations can occur (Fig. 5 A), and our model predicts a hump-shaped curve (Fig. 5 B, blue line). Thus, using our mathematical model, we predicted distinct, unmistakably discernable

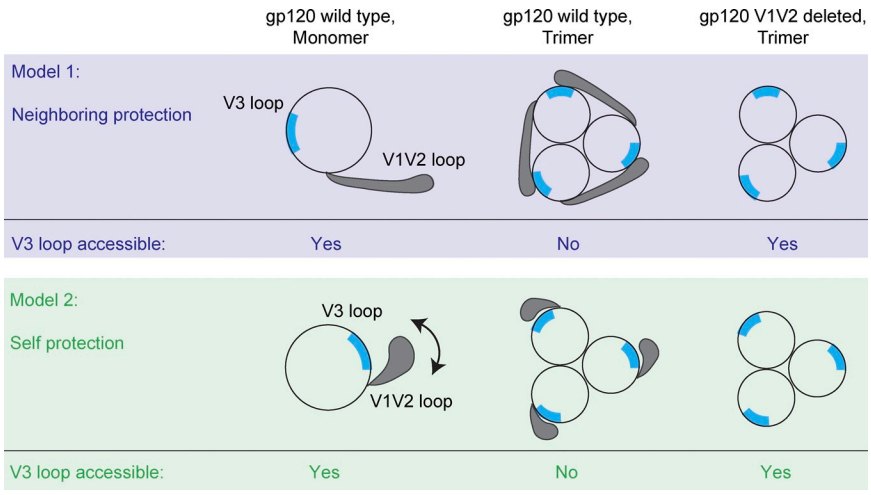

Figure 4. Self and neighboring protection scenarios of the V1V2 loop. The V1V2 loop can theoretically shield the V3 loop by neighboring protection (model 1), in which the V3 loop of a neighboring gp120 subunit is protected, or by self protection (model 2), in which the V3 loop of the own subunit is protected. Circles denote gp120 monomers. Blue rectangles denote the V3 loop. Gray shaded areas depict the V1V2 loop.

binding reactivity patterns for the self and neighboring protection scenarios.

We next probed our model experimentally and assessed mAb 19b binding to 11 different cell populations expressing varying compositions of heterotrimers composed of Env's NL4-3ΔV1V2 (lacking the V3 loop mAb epitope) and JR-FL* (harboring the V3 loop mAb epitope; Fig. 5 C). The data provided a strikingly clear pattern: 19b binding followed a hump-shaped curve, suggesting that neighboring protection is the mode by which the V1V2 domain shields the V3 loop. The same pattern of reactivity was observed for a second V3 loop mAb, 1-79. Of note, our approach relies on a random formation of heterotrimers. As the experiment depicted in Fig. 5 C necessitates two genetically divergent Env proteins to associate into trimers, we repeated these experiments with two alternate Env pairings that only differed in their V3 loop sequence and the presence and absence of the V1V2 loop (Fig. 5, D and E). In both instances, we again observed a hump-shaped reactivity pattern for mAbs 19b (Fig. 5, D and E) and 1-79 (Fig. 5 E), supporting the notion that both genetically divergent and closely related Env subunits form heterotrimers.

We further verified the V1V2 protection modus by assessing an alternate trimer scenario (setup 2) in which the 19b epitope is exposed on the V1V2-deleted Env protein, whereas the WT Env is resistant to 19b (Fig. 6, A–C). In this scenario, our model predicts reactivity patterns that are less divergent as binding in both settings is possible. If the self protection scenario holds true, our model predicts a straight line, and if

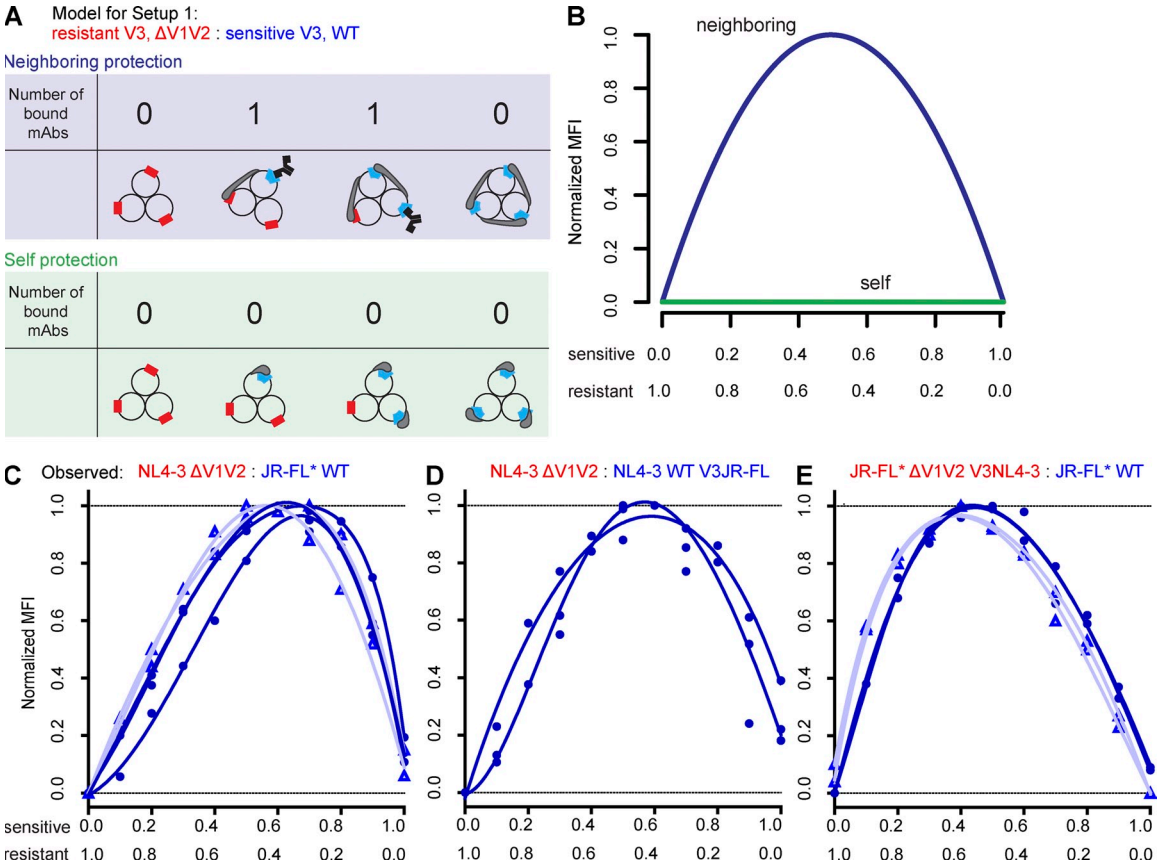

Figure 5. Dissection of self and neighboring protection scenarios of the V1V2 loop using mathematical modeling and empirical binding experiments to Env trimers. V1V2 loop shielding of the V3 loop was studied by binding of the V3 loop–specific mAbs 19b and 1-79 to heterogenous Env trimers that differ in V3 loop epitope presentation. Heterotrimer-expressing cells are generated by cotransfection of two different Env genes: a WT Env that is sensitive to the V3 loop mAbs and a V1V2-deleted Env (ΔV1V2) that carries a resistant V3 loop. (A) The schematic indicates the theoretical number of V3 loop mAb–accessible epitopes for all potential heterotrimer conformations assuming either self (green shaded area) or neighboring protection (blue shaded area) for the two respective Env's. Blue squares denote V3 loops sensitive to mAbs 19b and 1-79, and red squares denote resistant Env's. Gray shaded areas indicate V1V2 loops. (B) Predicted binding curves (MFI) for V3 loop mAbs under the binding scenarios depicted in A using our mathematical model. Green denotes self and blue denotes neighboring protection. Ratios of resistant to WT Env proteins are indicated on the x axis. (C–E) Experimental binding data. mAb 19b (circles) and 1-79 (triangles) binding to cells expressing the indicated heterotrimers at varying ratios was studied by FACS. Data of two to three independent experiments are shown. The highest MFI measured in each experiment was set as the maximum fluorescence level (100%), and measured MFI signals were normalized to the percentage of maximum fluorescence (% max). Dotted lines correspond to the minimum and maximum fluorescence levels (0 adn 100%). Unprocessed MFI data for mAbs 19b and 2G12 (to monitor total Env expression) are depicted in Fig. S2.

the neighboring protection holds true, we predict a convex curve. Experimental probing retrieved a convex-shaped reactivity pattern, again suggesting neighboring protection (Fig. 6 C).

Although our data carved out neighboring protection as the mode by which the V1V2 domain protects the V3 loop, we sought to further ascertain that our experimental approach is valid and is indeed capable of distinguishing between neighboring and self protection. Our approach depends on two key parameters: for one that heterotrimers form and, second, that heterotrimers consisting of WT and V1V2-deleted subunits adopt a conformation that resembles the WT-enabling V1V2 shielding to occur. Should the trimer assemble in a more open formation when WT and V1V2-deleted Env's are mixed, V1V2 shielding could be lost, allowing mAbs to access the V3 loop. To verify that heterotrimers form and have the appropriate conformation, we performed a control experiment (Fig. 7). Here, two identical Env's with a sensitive V3 loop that only differed in the presence/absence of the V1V2 loop were paired. When heterotrimers adopt the appropriate conformation and V1V2 shielding is intact, then irrespective of whether neighboring or self protection occurs, a linear increase in V3 loop mAb–accessible sites should be observed in this setup (Fig. 7, blue and green straight lines). In contrast, if heterotrimers assemble in a formation that jeopardizes V1V2 shielding, the V3 loop would be accessible in all heterotrimers, and the reactivity pattern in this case would dramatically shift to the left (Fig. 7 B, gray curve). Experimental probing revealed a straight line reactivity pattern, confirming that heterotrimers with intact shielding must form. These results verify that our model assumptions are correct and that neighboring and self protection can be dissected as described in setups 1 and 2 (Fig. 7).

To exclude the possibility that nonequal Env expression confounds our findings, gp120 expression levels on the various cell populations were monitored in all shielding experiments by assessing reactivities of the V3 loop mAb 19b and the carbohydrate-specific mAb 2G12 to control for V3 epitope and total gp120 Env expression, respectively (Fig. S2). Although Env expression varied to some extent between experiments and depended on the Env pairs studied, sufficient expression allowing assessment of mAb binding by FACS was achieved throughout. Fluctuations in Env expression levels are however unavoidable (Fig. S2; comparison of 2G12 binding to 100% sensitive and 100% resistant Env). As the observed differences were relatively small, we chose not to normalize the data by correcting for Env expression, as actual differences in Env expression and influences of differential mAb affinity for the heterologous Env pairs are difficult to tease apart. Importantly, variation in total Env expression levels was in all instances associated with a slight overexpression of one of the Env's, never with a decrease for cell populations that contain higher fractions of heterotrimers. From this, we conclude that the generated heterotrimers were stable and not genuinely prone to spontaneous gp120 shedding. The latter was important to verify as V1V2 shielding would not be effective on partially shed trimers and would report false positive signals in our system. We found that JR-FL*WT was expressed at slightly higher levels than NL4-3ΔV1V2 in most experiments, which corresponded with a modest rightward skew of the hump-shaped binding curves (Fig. 5 C). In an alternate

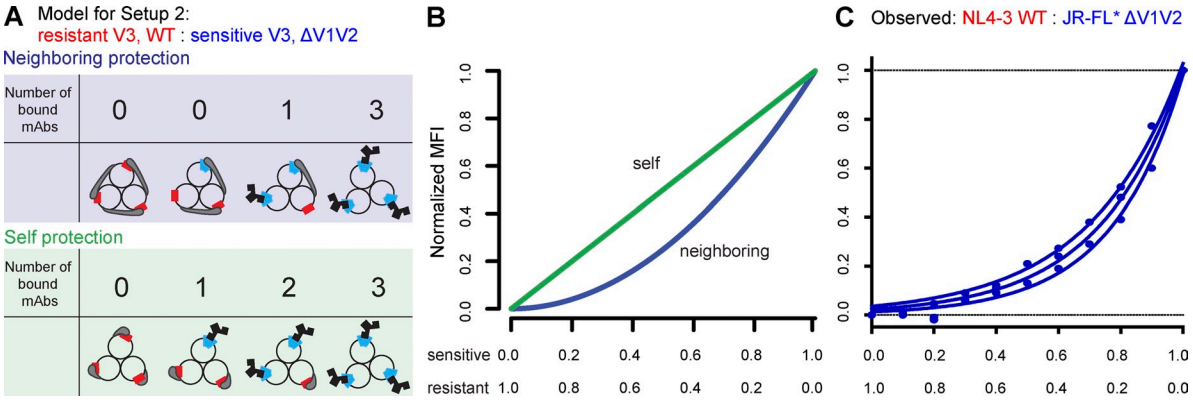

Figure 6. Dissection of self and neighboring protection in an alternate shielding scenario. V1V2 loop shielding of the V3 loop was studied by binding of the V3 loop–specific mAb 19b to heterogenous Env trimers that differ in 19b epitope presentation. Heterotrimer-expressing cells were generated by cotransfection of two different Env genes: a WT Env that is resistant to the V3 loop mAb (NL4-3) and a V1V2-deleted Env (ΔV1V2) that carries a 19b-sensitive V3 loop (JR-FL* ΔV1V2). (A) The schematic indicates the theoretical number of V3 loop mAb–accessible epitopes for all potential heterotrimer conformations assuming either self (green shaded area) or neighboring protection (blue shaded area) for the two respective Env's. Blue squares denote V3 loop sensitive to mAb 19b, and red squares denote resistant Env's. Gray shaded areas indicate V1V2 loops. (B) Predicted binding curves for V3 loop mAbs under the binding scenarios depicted in A using our mathematical model. Green denotes self and blue denotes neighboring protection. Ratios of resistant to WT Env proteins are indicated on the x axis. (C) Experimental binding data. mAb 19b (circles) binding to cells expressing the indicated heterotrimers at varying ratios was studied by FACS. Data of three independent experiments are shown. The highest MFI measured in each experiment was set as the maximum fluorescence level (100%), and measured MFI signals were normalized to the percentage of maximum fluorescence (% max). Dotted lines correspond to the minimum and maximum fluorescence levels (0 adn 100%). Unprocessed MFI data for mAbs 19b and 2G12 (to monitor total Env expression) are depicted in Fig. S2.

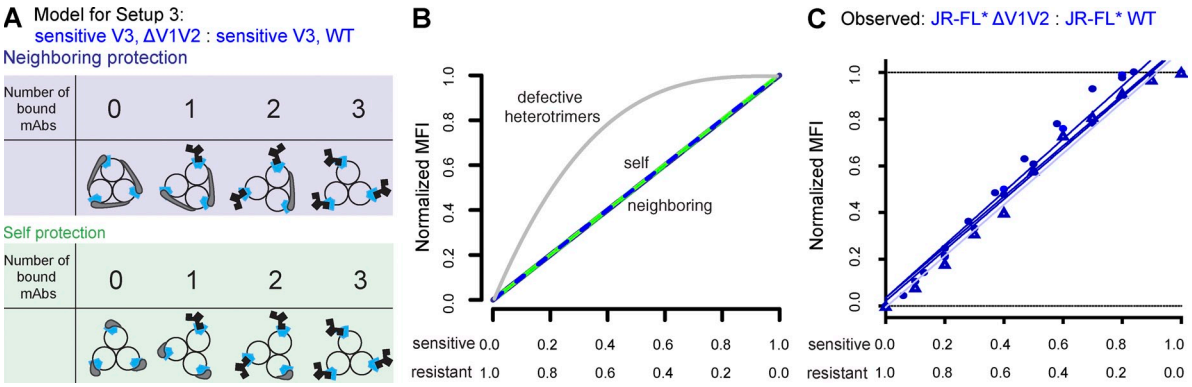

Figure 7. V1V2 loop shielding is intact in heterotrimers consisting of WT and V1V2-deleted subunits. (A–C) The capacity of the V1V2 loop to shield the V3 loop was assessed by studying binding of the V3 loop–specific mAbs 19b and 1-79 to chimeric Env trimers expressed on transfected 293-T cells. Env subunits used to generate the heterotrimers differed only in the presence/absence of the V1V2 loop. (A) Schematics indicating the theoretical number of 19b- and 1-79–accessible epitopes for all potential heterotrimer conformations assuming either self (green shaded area) or neighboring protection (blue shaded area) for the two indicated Env pairs. Blue squares denote V3 loop sensitive to mAbs 19b and 1-79. Gray shaded areas indicate V1V2 loops. (B) Predicted binding curves for V3 loop mAbs under the binding scenario depicted in A using our mathematical model. Green denotes self and blue denotes neighboring protection when heterotrimers are intact and confer V1V2 shielding. The gray line indicates the predicted binding pattern if heterotrimers have lost the capacity for V1V2 shielding. By varying expression ratios of the two respective Env proteins (indicated on the x axis), cell populations with higher or lower degree of heterotrimer conformations can be formed and are used in our model to predict binding patterns. (C) Experimental binding data. 19b (circles) and 1-79 (triangles) binding to 293-T cells expressing the indicated heterotrimers at varying ratios (indicated on the x axis) was studied by flow cytometry. Data of three independent experiments are shown. The highest MFI measured in each experiment was set as the maximum fluorescence level (100%), and measured MFI signals were normalized to the percentage of maximum fluorescence (% max). Dotted lines correspond to the minimum and maximum fluorescence levels (0 adn 100%). Unprocessed MFI data for mAbs 19b, 1-79, and 2G12 (to monitor total Env expression) are depicted in Fig. S2.

pairing, JR-FL*ΔV1V2$^{V3NL4-3}$ was expressed at higher levels than JR-FL*WT, which is consistent with a modest leftward skew of the binding pattern observed in Fig. 5 E. Thus, nonequal expression levels may in part cause slight, off-center skewing of the hump-shaped reaction patterns.

In a series of additional modeling approaches, we verified the influence of further parameters on our shielding assay to rule out the possibility that other confounding factors exist that affect our analysis and conclusions. In a first approach, we probed whether nonrandom trimer formation (i.e., preferential homotrimer formation) could affect our experimental approach. However, mathematical modeling of the potential influence of homotrimers on the hump-shaped reactivity pattern confirmed that, regardless of the frequency by which homotrimers are generated, no shift in the reactivity pattern can occur as mAb binding in this scenario completely depends on heterotrimer formation (Fig. S3 A). In this sense, our experimental approach provides also a formal proof that heterotrimer formation occurs.

Although we found that skewing of the hump-shaped reaction pattern cannot be explained by preferential homotrimer formation, this could affect the alternate shielding scenario (setup 2) to some extent and needs to be factored in when solely this protection scenario is used for assessments (Fig. 6 and Fig. S3 B). Of note, the influence of homotrimer formation cannot be assessed in the protection scenario studied in setup 3 (Fig. 7 and Fig. S3 C).

Besides intact trimers, partially shed spikes composed of gp120 dimers or monomers or solely gp41 stumps are expressed on infected or Env-transfected cells and virions (Moore et al., 1990; Moore et al., 2006; Ruprecht et al., 2011). In the context of monomers or dimers, V3 loops will not be, or only imperfectly, shielded (Fig. 2). As V3 loop mAb binding to monomers and dimers could influence our readout, we modeled the potential influence of partially shed spikes in our shielding analysis. We found that the presence of monomers and dimers induces a small rightward skew of the hump-shaped binding pattern (Fig. S3 D), which could add to the observed skewing in some of our experiments (Fig. 5 C). Monomer and dimer binding could also potentially influence the binding pattern in the alternate shielding scenarios (Figs. 6 and 7), although to an even smaller extent (Fig. S3, E and F).

In summary, we conclude that our experimental approach to uncover the mechanistic basis of V1V2 loop shielding is very robust. Small deviations from the in silico–derived reactivity patterns can occur when shielding is probed in vitro. However, these differences are marginal and are accounted for by differences in Env expression levels and the presence of monomeric and dimeric gp120 on the transfected cells.

DISCUSSION

Advances in recent years have highlighted the significant impact of the V1V2 domain on steering the sensitivity to antibody neutralization (Cao et al., 1997; Chackerian et al., 1997; Fox et al., 1997; Morikita et al., 1997; Stamatatos and Cheng-Mayer, 1998; Ly and Stamatatos, 2000; Losman et al., 2001; Johnson et al., 2003; Cole et al., 2004; Pinter et al., 2004; Pugach et al., 2004; Krachmarov et al., 2005, 2006; Saunders et al., 2005; Sagar et al., 2006; Shibata et al., 2007; Ching et al., 2008). Collectively, these studies point toward

very effective epitope masking by the V1V2 loop. The observation that currently circulating HIV strains have evolved their V1V2 domain to gain in neutralization resistance (Bunnik et al., 2010) supports the notion that the V1V2 loop provides an essential barrier for neutralizing antibodies elicited in natural infection. We reasoned that the protective effect of the V1V2 must be dominant to allow for such a focused evolution. Indeed, as we show in this study, the V1V2 domain has a tremendous capacity to protect against the humoral immune response elicited in vivo. The effect was particularly pronounced for more neutralization-resistant, primary tier 2 and 3 isolates, whereas neutralization-sensitive strains, as used in previous assessments of the V1V2 shielding effect (Morikita et al., 1997; Ly and Stamatatos, 2000; Losman et al., 2001; Pinter et al., 2004; Pugach et al., 2004; Krachmarov et al., 2005, 2006; Ching et al., 2008; Bontjer et al., 2009), underappreciated its magnitude. Unmasking of V1V2-protected domains unraveled a potent neutralization activity ubiquitously elicited in chronic infection across genetic subtypes. Most intriguingly, we found that this neutralizing activity was to a large extent conferred by V3 loop–specific antibodies, which cross-reacted with genetically divergent R5 V3 loop domains but not an X4 V3 loop. As the investigated chronic infection cohort did not include late stage infection, the lack of X4 cross-reactivity may reflect the predominance of R5 strain infections at the explored disease stage. mAb studies supported the tremendous impact of the V1V2 on shielding the V3 loop (Ly and Stamatatos, 2000; Losman et al., 2001; Krachmarov et al., 2005, 2006). However, our results also highlight shielding effects of the V1V2 on other neutralization-sensitive domains, further supporting its role as a broadly active barrier for neutralization in the context of the native trimer.

To date, the molecular basis of the V1V2 shielding capacity remains uncertain, largely as high-resolution structural information of the loop orientation in the context of intact HIV trimers is not available. Recent cryo-ET studies suggest that V1V2 and V3 loops may interact in the apex of trimeric Env spikes (White et al., 2010; Hu et al., 2011). In this study, we report on a structure–function analysis based on a specifically devised mathematical model and an experimental strategy to probe the theoretical assumptions. By studying V3 loop accessibility in the context of heterogeneous Env trimers composed of gp120 units with or without the V1V2 domain, we were able to demonstrate that the V1V2 loop protects the V3 loop of a neighboring gp120 in the context of the native trimer. Thus, the HIV-1 Env trimer adopts a quaternary structure that effectively shields highly cross-neutralization–sensitive domains by enforcing intersubunit contact through the V1V2 domain.

Further analysis will be needed to define whether and how increases in length and glycosylation within the V1V2 steer the efficacy of the intersubunit interaction and thus potentially improve shielding. However, a meaningful dissection of the contribution of sequence changes, glycosylation patterns, and length variation on V1V2 functionality will depend on the availability of crystal structure data of the V1V2 domain, as naturally occurring and artificially induced structural rearrangements upon sequence variation must be carefully evaluated in this type of analysis. The latter holds particularly true when the contribution of glycosylation is evaluated as removal of the specific potential N-linked glycosylation site necessitates changes in the amino acid backbone, which by themselves may cause structural rearrangements. In our current study, we explored the V1V2 shielding modus in the context of a neutralization-sensitive, tier 1 Env, NL4-3, and a relatively neutralization-resistant, tier 2 Env, JR-FL. Although V1V2 domains of these Env's differ in their degree of glycosylation, both were capable of protecting the adjacent gp120 molecule's V3 loop in the context of the trimer. The latter supports the notion that the V1V2 domain has an intrinsic capacity to confer protection throughout all disease stages and is, albeit at a lower level, also active in the setting of tier 1 viruses (Fig. S2).

Although our study does not provide data on the physical structure of the V1V2 domain per se, it offers new information on the quaternary organization of the V1V2 loop in the context of the Env trimer. The results of our analysis fit well with currently available structural data of gp120 and proposed models of the quaternary geometry of gp120 subunits within the trimeric spike (Kwong et al., 1998, 2000; Chen et al., 2005; Huang et al., 2005; Zanetti et al., 2006; Zhu et al., 2006; Liu et al., 2008a; Chen et al., 2009; Diskin et al., 2010; Finzi et al., 2010; Kong et al., 2010; Pancera et al., 2010; White et al., 2010; Xiang et al., 2010; Hu et al., 2011). A potential interaction of the V1V2 domain with the adjacent monomer's V3 loop has been considered for long (Kwong et al., 2000; Chen et al., 2005) but until to date could not be confirmed in the absence of the definition of a high-resolution trimer structure. Of note, results from recent cryo-ET studies of HIV Env spikes appear compatible with an interaction of V1V2 and V3 loops of neighboring subunits on the tip of the spike, but these analyses yet lack in resolution to unambiguously confirm such an interaction (Liu et al., 2008a; White et al., 2010; Hu et al., 2011). Our study confirms the proximity of the V1V2 and V3 loops of neighboring gp120 subunits within the trimeric spike and thus aids in validating the current models of Env trimer structure. By formally defining the orientation of the V1V2 loop toward the neighboring subunit in the trimer, our data close an important gap in the understanding of the structural architecture of the trimeric spike and provide a molecular basis on how the V1V2 masks neutralization-sensitive domains.

MATERIALS AND METHODS

Reagents and clinical specimen. Antibodies used in this study were made available by J. Robinson (Tulane University Medical Center, New Orleans, LA), M. Nussenzweig (The Rockefeller University, New York, NY), D. Burton (The Scripps Research Institute, La Jolla, CA), H. Katinger (Polymun Scientific, Vienna, Austria), S. Zolla-Pazner (New York University School of Medicine, New York, NY), J. Mascola (Vaccine Research Center, National Institutes of Health, Bethesda, MD), and the AIDS Research and Reference Reagent Program (Division of AIDS, National Institute of Allergy and Infectious Diseases, National Institutes of Health). The precise origin and epitope specificities of mAbs used in this study are listed in Table S2.

Plasma samples were obtained from individuals with chronic HIV-1 infection (>6 mo infected) enrolled in (a) the Swiss HIV Cohort Study (Schoeni-Affolter et al., 2010), (b) the Zurich Primary HIV Infection Study (Rieder et al., 2010), and (c) the Swiss Spanish Treatment Interruption trial (Trkola et al., 2004). All experiments were approved by the ethics committee of the University Hospital Zurich, and written informed consent was obtained from all individuals. Detailed patient demographics are listed in Table S3. Peptides were provided by J. Robinson and T. Riedel (University of Zurich, Zurich, Switzerland).

Cells. 293-T and TZM-bl cells were obtained from the American Type Culture Collection and the National Institutes of Health AIDS repository, respectively, and cultured as described previously (Rusert et al., 2009).

HIV Env genes. All HIV Env genes used in this study have been previously described (Table S1) with the exception of the Env ZA110.C.10.14, which was previously isolated in our laboratory from a rapidly progressing individual during chronic infection (Table S1).

Generation of V1V2-deleted Env's. An overview of all mutant Env genes generated in the frame of this study is provided in Table S1. For the construction of V1V2-deleted viruses, the natural restriction sites DraIII (upstream) and StuI (downstream) of the V1V2 were used to substitute the original V1V2 domain with a 3-aa linker sequence DAG as described previously (Fig. S1 A; Bontjer et al., 2009). Env's were cloned into the expression vector pcDNA 3.1. DraIII and StuI restriction sites in pcDNA 3.1 were removed before construction of the V1V2 mutant viruses. The integrity of the derived mutant Env's was verified by sequencing, and functionality was ascertained in a pseudotype virus infection assay. All Env mutants proved infection competent in pseudotype infection upon V1V2 deletion/DAG insertion. As expected, infectivity upon V1V2 deletion decreased to some extent compared with the corresponding WT isolates. However, for all Env's described here, this reduction was <10-fold, and infectivity was in all cases sufficient for inhibitor experiments. The only exception was the Env of JR-FL as this protein did not tolerate the substitution by its cognate V1V2 linker sequence. However, we were able to restore its infectivity by introducing a D197N mutation that generates an additional potential N-glycosylation site downstream of the V1V2. We designated this virus as ΔV1V2JR-FL* and constructed a corresponding WT JR-FL derivative harboring the D197N mutation (designated JR-FL*). This modification proved to have no influence on the neutralization sensitivity of the virus as we found that both JR-FL and JR-FL* had identical sensitivity to neutralization by mAbs and patient plasma.

To generate V3 loop–swapped NL4-3 and JR-FL* Env's, an overlap extension PCR was used. The NL4-3 and JR-FL* Env sequences upstream of the V3 loop (NL4-3 primers, 5′-GAGACAGCGACGAAGAGCTCCTC-3′ and 5′-GGGTCTTGTACAATTAATTTCTACAG-3′; JR-FL* primers, 5′-CTCAAGACAGTCAGACTCATCTTGC-3′ and 5′-GTATTGTTGTTGGGTCTTGTACAATTAATTTC-3′), the individual V3 loops (NL4-3 primers, 5′-GTACAAGACCCAACAACAATACAAG-3′ and 5′-GTTACAATGTGCTTGTCTCATATTTCC-3′; JR-FL* primers, 5′-CTGTAGAAATTAATTGTACAAGACCC-3′ and 5′-GCTCTACTAATGTTACAATGTGC-3′), and the NL4-3 and JR-FL* Env sequences downstream of the V3 loop (NL4-3 primers, 5′-GCACATTGTAACATTAGTAGAGC-3′ and 5′-TTTTGACCACTTGCCACCCATCTTATAGC-3′; JR-FL* primers, 5′-TATGAGACAAGCACATTGTAACATTAGTAGAGC-3′ and 5′-ACTTTTTGACCACTTGCCACCC-3′) were amplified in separate PCR reactions. Subsequently, the NL4-3 and JR-FL* Env upstream fragments were mixed with the desired V3 loop fragment and subjected to a first overlap extension PCR followed by purification of the fusion products by gel extraction. The purified fusion products were subjected to a second overlap extension PCR with the Env downstream fragments that correspond to the upstream fragment yielding the desired chimeric Env gene. The final fusion products were gel purified and cloned into pcDNA3.1. The sequence of the derived mutant Env's was verified, and epitope accessibility was probed by FACS. Env JR-FL*ΔV1V2_V3^{NL4-3} proved not infectious, whereas NL4-3WT_JR-FL^{V3} was infectious in the context of pseudovirus infection.

Virus preparation. Env-pseudotyped viruses were prepared by cotransfection of 293-T cells with the plasmids encoding the respective Env genes and the luciferase reporter HIV vector pNLluc-AM as described previously (Rusert et al., 2009).

Neutralization assay using Env-pseudotyped virus. The neutralization activity of mAbs and patient plasma was evaluated on TZM-bl cells as described previously (Rusert et al., 2009). Virus input was chosen to yield virus infectivity corresponding to 5,000–20,000 RLU (relative light units) in the absence of inhibitors. The antibody concentrations or reciprocal plasma titers causing 50% reduction in viral infectivity (inhibitory concentration IC_{50} or neutralization titer NT_{50}) were calculated by fitting pooled data from two to three independent experiments to sigmoid dose–response curves (variable slope) using Prism software (GraphPad Software). If 50% inhibition was not achieved at the highest or lowest drug or plasma concentration, a greater than or less than value was recorded.

Neutralization assay in the presence of competing linear V3 loop peptides. Neutralization assays were performed in the presence of linear peptides compromising the aa 301–324 (HxB2) of the corresponding V3 loop: JR-FL–V3, NNTRKSIHIGPGRAFYTTGEIIG; NL4-3–V3, NNTRKSIRIQRGPGRAFVTIGKIG; SF162-V3, NNTRKSITIGPGRAFYATGDIIG; and c10.14-V3, NNTRRSIHIGPGKAFYTGGIIG. We used a fixed concentration of 10 μg/ml of the V3 peptides in all experiments. This dose of V3 peptide was sufficient to completely compete off neutralization activity of the V3 loop–specific mAb 19b against JR-FL*ΔV1V2 at mAb concentrations of 50 μg/ml. None of the probed peptides directly influenced the infectivity of the probed R5 and X4 viruses, and murine leukemia virus Env–pseudotyped virus was used as control. Patient plasma samples were preincubated with the corresponding V3 loop peptides for 1 h. Then virus was added, and the mixture was preincubated for a further 1 h before infection of TZM-bl cells. The final, lowest dilution of the plasma sample probed was 1:200. 50% inhibitory concentration and neutralization activity in the presence and absence of competing V3 loop peptide were determined.

Antibody binding to monomeric gp120. Sequences encoding gp120 WT and gp120ΔV1V2 proteins were derived from full-length Env genes and cloned into the expression vector CMV-R (provided by P. Kwong [Vaccine Research Center, National Institutes of Health]). Protein was generated upon transfection of FreeStyle 293 cells (Invitrogen). In brief, 1–10^6/ml cells in a total volume of 100 ml of 293 FreeStyle medium (Invitrogen) were transfected with 160 μg DNA and 320 μg polyethyleneimine. gp120-containing supernatant was harvested on days 3 and 5 and used for binding experiments by ELISA. To this end, gp120 proteins were immobilized on ELISA plates coated with sheep antibody D7324 directed to the C5 domain of gp120 (Aalto). Plasma IgG titers and mAb to gp120 were determined by ELISA as described previously (Trkola et al., 2004). Midpoint titers were defined by fitting dose-dependent curves with a variable slope by Prism software. Each individual sample was controlled for unspecific binding activity (binding in absence of gp120), and data was corrected for unspecific binding before 50% binding titers or concentrations were derived. Curve fitting was constrained at 0% but not at 100% binding because plasma and mAbs show comparable but not equal saturation levels. In rare cases, anti-gp120 antibody titers in plasma were too low to reach binding saturation. To assess binding efficacy in these cases, maximal binding was set as the mean level of maximal binding observed in the 83 plasma samples, and curve fitting was performed using this mean level as 100% binding. To calculate the 50% binding titers, curves were fitted through the pooled data from two to three independent assays.

Mathematical model to dissect self and neighboring protection modes of the V1V2 loop. We developed a mathematical model with the aim to dissect experimentally whether neighboring or self protection is the mode by which the V1V2 loop protects against neutralization. Our theoretical and experimental approach is based on studying heterogeneous trimers composed of two different Env proteins. These Env proteins must differ in

two regions. The first region concerns the V1V2 loop and the second region an antibody epitope (in our case the epitope of the V3 loop–specific antibodies 19b and 1-79), which is presumably masked by the V1V2 loop. We engineered Env proteins in which the V1V2 loop is either present or deleted, and 19b and 1-79 V3 loop mAb epitopes are present or defective (naturally or engineered). Two experimental setups with two different Env proteins out of the total eight possible combinations with these four Env variations can be used to distinguish between neighboring and self protection: (1) one Env protein contains the V1V2 loop and is sensitive to antibody binding, whereas the other Env protein is V1V2 deleted and antibody binding resistant; (2) one Env protein contains the V1V2 loop and is resistant to antibody binding, whereas the other Env protein is V1V2 deleted and antibody binding sensitive.

The schematic in Fig. 5 A shows how many antibodies could bind to the different trimers depending on the mechanism of protection in the experimental setup 1, and Fig. 6 A shows the number of trimers binding to the different trimers in setup 2. As a control experiment, we also studied an experimental setup (setup 3) in which two homologue antibody binding–sensitive Env proteins were mixed that only differed in the presence and absence of the V1V2 loop. This setup does not allow us to distinguish between neighboring and self protection but instead allows us to validate the integrity of heterotrimer formation. Fig. 7 A illustrates how many antibodies can bind to the different trimer types that can form in this setup.

In our experiments, we seek to determine the accessibility of the V3 loop on trimers by determining the binding efficacy of the given V3 loop mAbs by deriving the mean fluorescent intensity (MFI) of fluorophore-labeled mAb binding by FACS.The MFI is proportional to the number of antibodies binding to the Env-expressing cells. To predict the MFI, we need to average the number of bound antibodies over all trimer types in a cell population. This requires us to factor in the frequency of each trimer type, which depends on the fraction of different Env proteins. Let us define f_{bs} as the fraction of Env proteins with a binding-sensitive epitope (independent of whether it is protected by a V1V2 loop). Under the assumption that the different Env proteins trimerize perfectly randomly, the probability that a trimer consists of i Env proteins with an antibody binding–sensitive epitope and $3 - i$ antibody-resistant Env proteins is

$$\binom{3}{i} f_{bs}^{i} \left(1 - f_{bs}\right)^{3-i}.$$

For setup 3, all Env proteins are binding sensitive. For this setup, we introduce the parameter f_{Δ} that denotes the fraction of Env proteins without V1V2. The frequencies of each trimer type are given by the same formula as above with f_{Δ} instead of f_{bs}.

The number of antibodies binding to an average trimer can be calculated by summing over the products of the number of antibodies binding to a specific trimer (determined in Figs. 5 A, 6 A, and 7 A) and the probability that this trimer is formed. Table I lists the number of antibodies binding to an average trimer for each experimental setup and mode of protection.

To be able to compare our mathematical prediction with the observed MFI, we normalize the MFI and the expressions in Table I such that its maximum over the various levels of f_{bs} is 1. Thus, we obtained mathematical expressions that predict the behavior of the normalized MFI as a function of the fraction of antibody-sensitive Env proteins, f_{bs}. These predictions are shown in Figs. 5 B, 6 B, and 7 B.

Setup 3 does not allow us to distinguish between neighboring and self protection as identical reactivity patterns are predicted for both instances. Instead, setup 3 allows us to derive information on whether or not the formed heterotrimers adopt an appropriate conformation that enables V1V2 shielding to occur. Should the formed heterotrimers disable V1V2 shielding, the V3 loop would become accessible. In this case, MFI reactivity patterns would change substantially and follow the function

$$3 \times 3 f_{\Delta} \left(1 - f_{\Delta}\right)^{2} + 3 \times 3 f_{\Delta}^{2} \left(1 - f_{\Delta}\right) + 3 \times f_{\Delta}^{3}.$$

Modeling the influence of segregation (preferential homotrimer formation) on the reactivity pattern in the shielding assay. In the segregation model, we assume that the formation of homotrimers is more likely than that of heterotrimers. To assess the potential impact of Env protein segregation, we introduced a segregation parameter, $0 \le \xi \le 1$, into our basic model. $\xi = 0$ corresponds to no segregation, and $\xi = 1$ corresponds to complete segregation. Table II lists the number of antibodies that bind, on average, to a trimer with segregation.

The probabilities to form a trimer with i binding–sensitive Env proteins, P_i, appearing in Table II are defined according to the segregation model in Magnus and Regoes (2010) as

$$P_1 = f_{bs} \left(1 - f_{bs}^{1-\xi}\right)^{2} + 2\left(1 - f_{bs}\right)\left(1 - f_{bs}\right)^{1-\xi} \left(1 - \left(1 - f_{bs}\right)^{1-\xi}\right),$$

$$P_2 = 2 f_{bs} f_{bs}^{1-\xi} \left(1 - f_{bs}^{1-\xi}\right) + \left(1 - f_{bs}\right)\left(1 - \left(1 - f_{bs}\right)^{1-\xi}\right)^{2}, \quad \text{and}$$

$$P_3 = f_{bs}^{3-2\xi}.$$

For setup 3, f_{bs} must be replaced by f_{Δ} to obtain the probabilities P_i. As the V3 loop is only accessible on heterotrimers in the shielding scenario studied in Fig. 5 (setup 1; hump-shaped curve), homotrimer formation, regardless of its extent, is not predicted to influence the normalized MFI. In the alternate shielding scenario (setup 2; Fig. 6), the V3 loop can be accessed on heterotrimers, and their influence, although small, must be considered (Fig. S3 B).

Modeling the influence of gp120 monomers and dimers on the reactivity pattern in the shielding assay. Additionally to intact trimeric Env spikes, partially shed Env spikes displaying gp120 monomers and dimers will be expressed on the cell surface of Env-transfected cells. V1V2 shielding on these partially shed spikes will not be effective, and the V3 loop will thus be accessible. With what frequency monomers and dimers form is not known. Assay variations (e.g., transfection and expression efficiencies) can be envisaged to play a role. The fraction of Env monomers and dimers may also differ depending on the Env proteins involved. The stability of homo- and heterotrimers may differ, rendering one more prone to spontaneous gp120 shedding than the other. The latter

Table I. Mathematical models for the number of antibodies bound per trimer

Setup	Neighboring protection	Self protection
1	$1 \times 3 f_{bs} \left(1 - f_{bs}\right)^{2} + 1 \times 3 f_{bs}^{2} \left(1 - f_{bs}\right)$	0
2	$1 \times 3 f_{bs}^{2} \left(1 - f_{bs}\right) + 3 \times f_{bs}^{3}$	$1 \times 3 f_{bs} \left(1 - f_{bs}\right)^{2} + 2 \times 3 f_{bs}^{2} \left(1 - f_{bs}\right) + 3 \times f_{bs}^{3}$
3	$1 \times 3 f_{\Delta} \left(1 - f_{\Delta}\right)^{2} + 2 \times 3 f_{\Delta}^{2} \left(1 - f_{\Delta}\right) + 3 \times f_{\Delta}^{3}$	$1 \times 3 f_{\Delta} \left(1 - f_{\Delta}\right)^{2} + 2 \times 3 f_{\Delta}^{2} \left(1 - f_{\Delta}\right) + 3 \times f_{\Delta}^{3}$

Table II. Mathematical models for the number of antibodies bound per trimer under the consideration of Env protein segregation

Setup	Neighboring protection	Self protection
1	$1 \times P_1 + 1 \times P_2$	0
2	$1 \times P_2 + 3 \times P_3$	$1 \times P_1 + 2 \times P_2 + 3 \times P_3$
3	$1 \times P_1 + 2 \times P_2 + 3 \times P_3$	$1 \times P_1 + 2 \times P_2 + 3 \times P_3$

would cause fluctuations in the expression levels of monomers and dimers but also the total Env content of the cell as a substantial proportion of the Env proteins will be released and thus lost for analysis. In the event that heterotrimers dissociate at a higher frequency than homotrimers, total Env expression levels should be lower at those Env ratios where the highest heterotrimer formation is to be expected ($f_{bs} = 0.5$). We have controlled for Env expression in each individual experiment by assessing the capacity of mAb 2G12 to bind to cell surface–expressed Env's. This mAb recognizes monomeric, dimeric, and trimeric gp120 and is largely unaffected by the presence of V1V2 and the mutations in V3 studied here. Based on 2G12 reactivity, we were able to exclude the possibility that the studied heterotrimers are inherently instable and promote spontaneous shedding and thus monomeric and dimeric gp120 formation. Env concentration was comparable at all Env ratios studied. Should a heterotrimer be instable, total Env content as measured by 2G12 would be lower in cell populations that contain a higher heterotrimer content (e.g., $f_{bs} = 0.5$).

However, as some degree of spontaneous shedding will occur regardless of what specific Env is studied, we had to evaluate the effect of antibody binding to gp120 monomers and dimers in our assay system. To assess the potential impact of monomers and dimers on our prediction of the normalized MFI, we assumed that the total number of gp120 monomers and dimers expressed on a transfected cell is the same for all investigated cell populations. For setup 1 and 2, we assumed that one antibody binds to a binding-sensitive Env monomer, one antibody binds to a heterodimer (consisting of one V3 loop–sensitive and one resistant Env), and two antibodies bind to a homodimer consisting of two binding sensitive Env's. In the case of setup 3, two antibodies are assumed to bind to heterotrimers. Monomers are expressed at a rate a, and dimers of either type are expressed at a rate b. Under these assumptions, we simply have to add the terms af_{bs} for antibodies binding to monomers and a term for the binding to dimers, which, for setup 1 and 2, is $b(2f_{bs}(1 - f_{bs}) + 2f_{bs}^2)$, or, for setup 3, $b(4f_{bs}(1 - f_{bs}) + 2f_{bs}^2)$, to the expressions in Table I. Upon simplification, we derived the following formulas for setup 1 and 2 under the consideration of monomer/dimer binding (Table III).

The parameter $c = a + 2b$ denotes the fraction of antibodies bound to monomers and dimers. If the neighboring protection scenario holds true, c can be estimated from the normalized MFI in setup 1 at the point $f_{bs} = 1$.

Experimentally probing self and neighboring protection modes of the V1V2 loop. 293-T cells seeded in 12-well tissue culture plates were transfected with 1.6 µg of the respective HIV Env–encoding plasmids and 0.4 µg of the rev-encoding plasmid pCMV-rev using jetPEI (Polyplus Transfection; Chemie Brunschwig AG) according to the manufacturer's instruction. To generate virions bearing heterogeneous Env trimers, two different Env-encoding plasmids were transfected. To vary the heterogeneous trimer composition, cells were transfected with different ratios of the two respective Env plasmids. In total, 11 ratios with the respective plasmids' concentration varying in 10% increments were probed (one Env ranging from 100% to 0%, the second ranging from 0% to 100% in the same cotransfection). The following Env genes were studied: Env's that carry the epitope of the V3 loop mAbs 19b and 1-79 (JR-FL*WT, JR-FL*ΔV1V2, and NL4-3WT_JR-FL^{V3}) and Env's that do not carry the 19b epitope (NL4-3WT, NL4-3ΔV1V2, and JR-FL*ΔV1V2_V3^{NL4-3}). The following pairs were investigated: (a) JR-FL*WT with NL4-3ΔV1V2 (Fig. 5 C), (b) NL4-3WT_JR-FL^{V3} with NL4-3ΔV1V2 (Fig. 5 D), (c) JR-FL*ΔV1V2_V3^{NL4-3} with JR-FL*WT (Fig. 5 E), (d) NL4-3WT with JR-FL*ΔV1V2 (Fig. 6 C), and (e) JR-FL*WT with JR-FL*ΔV1V2 (Fig. 7 C).

Cells were detached 48 h after transfection using PBS, 1% FCS, and 10 mM EDTA, and V3 loop accessibility was studied by monitoring the binding efficiency of the V3 loop mAbs 19b or 1-79 to the heterogeneous Env proteins expressed on the cells' surface. As control for equivalent Env expression of the heterotrimer, binding efficiency of the carbohydrate-specific mAb 2G12, which binds to all probed WT and Env mutants with comparable efficiency, was assessed in all experiments (Fig. S2). Stainings were performed with mAbs 19b and 1-79 and biotinylated mAb 2G12, and bound antibody was detected using Cy5-conjugated F(ab′)$_2$ goat anti–human IgG (Jackson ImmunoResearch Laboratories, Inc.) and streptavidin-APC (BioLegend), respectively. Viability stain propidium iodide (Invitrogen) was added to all samples 10 min before acquisition, and dead cells were excluded from analysis. Samples were acquired on a CyAn ADP Analyzer (Beckman Counter) and analyzed using FlowJo software (Tree Star). The highest MFI measured in each experiment was set as the maximum fluorescence level (100%), and measured MFI signals were normalized to the percentage of maximum fluorescence (% max).

Statistical analysis and data processing. All 50% neutralization, inhibition, or binding doses were determined by fitting a sigmoid dose–response curve with a variable slope through the pooled data of two to three independent assays. Error bars indicate the 95% confidence interval calculated by Prism software. Fold increases in plasma neutralization and binding activity refer to the difference between median activity of the 83 plasma samples against WT and V1V2-deleted Env's (Fig. 1). One-way analysis of variance with post-tests Tukey's multiple comparison and Newman Keuls was used to test whether the mean neutralization activity of the 83 patients' plasma measured against NL4-3ΔV1V2 is significantly different from the other ΔV1V2 viruses. The same test was used to compare the datasets after V3 peptide

Table III. Mathematical models for the number of antibodies bound per trimer under the consideration of monomer/dimer binding

Setup	Neighboring protection	Self protection
1	$3f_{bs}\left(1-f_{bs}\right)^2+3f_{bs}^2\left(1-f_{bs}\right)+cf_{bs}$	cf_{bs}
2	$1\times3f_{bs}^2\left(1-f_{bs}\right)+3\times f_{bs}^3+cf_{bs}$	$1\times3f_{bs}\left(1-f_{bs}\right)^2+2\times3f_{bs}^2\left(1-f_{bs}\right)+3\times f_{bs}^3+cf_{bs}$
3	$1\times3f_{\Delta}\left(1-f_{\Delta}\right)^2+2\times3f_{\Delta}^2\left(1-f_{\Delta}\right)+3\times f_{\Delta}^3+af_{\Delta}+4bf_{\Delta}-2bf_{\Delta}^2$	$1\times3f_{\Delta}\left(1-f_{\Delta}\right)^2+2\times3f_{\Delta}^2\left(1-f_{\Delta}\right)+3\times f_{\Delta}^3+af_{\Delta}+4bf_{\Delta}-2bf_{\Delta}^2$

competition (Fig. 3 B). To assess potential interdependencies between measured neutralization and binding activities, Pearson correlation parameters for 50% plasma neutralization or binding activities were assessed (Table S5).

Online supplemental material. Fig. S1 analyzes the shielding capacity of the V1V2 loop. Fig. S2 shows the analysis of mAb binding to viral Env on cell populations expressing varying composition of heterotrimers. Fig. S3 shows predictions for binding patterns in the shielding analysis considering model extensions for preferential homotrimer formation and the presence of monomeric and dimeric gp120 units. Table S1, included as an Excel file, shows an overview and characteristics of WT and chimeric HIV-1 Env's. Table S2, included as an Excel file, shows the origin and specificity of HIV-1–directed mAbs and entry inhibitors. Table S3, included as an Excel file, provides an overview of plasma samples from individuals with chronic HIV-1 infection used in this study. Table S4, included as an Excel file, depicts columns statistics of 50% plasma neutralization and binding titers reported in Fig. 1. Table S5, included as an Excel file, lists Pearson correlation analysis of 50% plasma neutralization and binding titers. Online supplemental material is available at http://www.jem.org/cgi/content/full/jem.20110196/DC1.

We thank Herbert Kuster and Therese Uhr for technical assistance and John Robinson and Tina Riedel for providing V3 loop peptides. We thank the patients participating in the clinical studies from which samples for the current study was derived. We gratefully acknowledge the Swiss HIV Cohort Study (SHCS) for access to samples and Jürg Böni for the use of the SHCS drug resistance database.

Support was provided by the Swiss National Science Foundation (grants 310000-120739 and 310030-135527 to A. Trkola, 315200-114148 to R.R. Regoes, and 324730-130865 to H.F. Günthard). A. Trkola is an Elizabeth Glaser Scientist supported by the Elizabeth Glaser Pediatric AIDS Foundation.

The authors declare no competing financial interests.

Submitted: 27 January 2011
Accepted: 4 May 2011

REFERENCES

Arthos, J., C. Cicala, E. Martinelli, K. Macleod, D. Van Ryk, D. Wei, Z. Xiao, T.D. Veenstra, T.P. Conrad, R.A. Lempicki, et al. 2008. HIV-1 envelope protein binds to and signals through integrin alpha4beta7, the gut mucosal homing receptor for peripheral T cells. *Nat. Immunol.* 9:301–309. doi:10.1038/ni1566

Bontjer, I., A. Land, D. Eggink, E. Verkade, K. Tuin, C. Baldwin, G. Pollakis, W.A. Paxton, I. Braakman, B. Berkhout, and R.W. Sanders. 2009. Optimization of human immunodeficiency virus type 1 envelope glycoproteins with V1/V2 deleted, using virus evolution. *J. Virol.* 83:368–383. doi:10.1128/JVI.01404-08

Bunnik, E.M., Z. Euler, M.R. Welkers, B.D. Boeser-Nunnink, M.L. Grijsen, J.M. Prins, and H. Schuitemaker. 2010. Adaptation of HIV-1 envelope gp120 to humoral immunity at a population level. *Nat. Med.* 16:995–997. doi:10.1038/nm.2203

Cao, J., N. Sullivan, E. Desjardin, C. Parolin, J. Robinson, R. Wyatt, and J. Sodroski. 1997. Replication and neutralization of human immunodeficiency virus type 1 lacking the V1 and V2 variable loops of the gp120 envelope glycoprotein. *J. Virol.* 71:9808–9812.

Chackerian, B., L.M. Rudensey, and J.C. Overbaugh. 1997. Specific N-linked and O-linked glycosylation modifications in the envelope V1 domain of simian immunodeficiency virus variants that evolve in the host alter recognition by neutralizing antibodies. *J. Virol.* 71:7719–7727.

Chen, B., E.M. Vogan, H. Gong, J.J. Skehel, D.C. Wiley, and S.C. Harrison. 2005. Structure of an unliganded simian immunodeficiency virus gp120 core. *Nature.* 433:834–841. doi:10.1038/nature03327

Chen, L., Y.D. Kwon, T. Zhou, X. Wu, S. O'Dell, L. Cavacini, A.J. Hessell, M. Pancera, M. Tang, L. Xu, et al. 2009. Structural basis of immune evasion at the site of CD4 attachment on HIV-1 gp120. *Science.* 326:1123–1127. doi:10.1126/science.1175868

Ching, L.K., G. Vlachogiannis, K.A. Bosch, and L. Stamatatos. 2008. The first hypervariable region of the gp120 Env glycoprotein defines the neutralizing susceptibility of heterologous human immunodeficiency virus type 1 isolates to neutralizing antibodies elicited by the SF162gp140 immunogen. *J. Virol.* 82:949–956. doi:10.1128/JVI.02143-07

Chohan, B., D. Lang, M. Sagar, B. Korber, L. Lavreys, B. Richardson, and J.C. Overbaugh. 2005. Selection for human immunodeficiency virus type 1 envelope glycosylation variants with shorter V1-V2 loop sequences occurs during transmission of certain genetic subtypes and may impact viral RNA levels. *J. Virol.* 79:6528–6531. doi:10.1128/JVI.79.10.6528-6531.2005

Cicala, C., E. Martinelli, J.P. McNally, D.J. Goode, R. Gopaul, J. Hiatt, K. Jelicic, S. Kottilil, K. Macleod, A. O'Shea, et al. 2009. The integrin alpha4beta7 forms a complex with cell-surface CD4 and defines a T-cell subset that is highly susceptible to infection by HIV-1. *Proc. Natl. Acad. Sci. USA.* 106:20877–20882. doi:10.1073/pnas.0911796106

Cole, K.S., J.D. Steckbeck, J.L. Rowles, R.C. Desrosiers, and R.C. Montelaro. 2004. Removal of N-linked glycosylation sites in the V1 region of simian immunodeficiency virus gp120 results in redirection of B-cell responses to V3. *J. Virol.* 78:1525–1539. doi:10.1128/JVI.78.3.1525-1539.2004

Derdeyn, C.A., J.M. Decker, F. Bibollet-Ruche, J.L. Mokili, M. Muldoon, S.A. Denham, M.L. Heil, F. Kasolo, R. Musonda, B.H. Hahn, et al. 2004. Envelope-constrained neutralization-sensitive HIV-1 after heterosexual transmission. *Science.* 303:2019–2022. doi:10.1126/science.1093137

Diskin, R., P.M. Marcovecchio, and P.J. Bjorkman. 2010. Structure of a clade C HIV-1 gp120 bound to CD4 and CD4-induced antibody reveals anti-CD4 polyreactivity. *Nat. Struct. Mol. Biol.* 17:608–613. doi:10.1038/nsmb.1796

Finzi, A., S.H. Xiang, B. Pacheco, L. Wang, J. Haight, A. Kassa, B. Danek, M. Pancera, P.D. Kwong, and J. Sodroski. 2010. Topological layers in the HIV-1 gp120 inner domain regulate gp41 interaction and CD4-triggered conformational transitions. *Mol. Cell.* 37:656–667. doi:10.1016/j.molcel.2010.02.012

Fox, D.G., P. Balfe, C.P. Palmer, J.C. May, C. Arnold, and J.A. McKeating. 1997. Length polymorphism within the second variable region of the human immunodeficiency virus type 1 envelope glycoprotein affects accessibility of the receptor binding site. *J. Virol.* 71:759–765.

Frost, S.D., Y. Liu, S.L. Pond, C. Chappey, T. Wrin, C.J. Petropoulos, S.J. Little, and D.D.C. Richman. 2005. Characterization of human immunodeficiency virus type 1 (HIV-1) envelope variation and neutralizing antibody responses during transmission of HIV-1 subtype B. *J. Virol.* 79:6523–6527. doi:10.1128/JVI.79.10.6523-6527.2005

Gorny, M.K., L. Stamatatos, B. Volsky, K. Revesz, C. Williams, X.H. Wang, S. Cohen, R. Staudinger, and S. Zolla-Pazner. 2005. Identification of a new quaternary neutralizing epitope on human immunodeficiency virus type 1 virus particles. *J. Virol.* 79:5232–5237. doi:10.1128/JVI.79.8.5232-5237.2005

Harrington, P.R., J.A. Nelson, K.M. Kitrinos, and R.C. Swanstrom. 2007. Independent evolution of human immunodeficiency virus type 1 env V1/V2 and V4/V5 hypervariable regions during chronic infection. *J. Virol.* 81:5413–5417. doi:10.1128/JVI.02554-06

Hu, G., J. Liu, K.A. Taylor, and K.H. Roux. 2011. Structural comparison of HIV-1 envelope spikes with and without the V1/V2 loop. *J. Virol.* 85:2741–2750. doi:10.1128/JVI.01612-10

Huang, C.C., M. Tang, M.Y. Zhang, S. Majeed, E. Montabana, R.L. Stanfield, D.S. Dimitrov, B. Korber, J. Sodroski, I.A. Wilson, et al. 2005. Structure of a V3-containing HIV-1 gp120 core. *Science.* 310:1025–1028. doi:10.1126/science.1118398

Johnson, W.E., H. Sanford, L. Schwall, D.R. Burton, P.W. Parren, J.E. Robinson, and R.C. Desrosiers. 2003. Assorted mutations in the envelope gene of simian immunodeficiency virus lead to loss of neutralization resistance against antibodies representing a broad spectrum of specificities. *J. Virol.* 77:9993–10003. doi:10.1128/JVI.77.18.9993-10003.2003

Kitrinos, K.M., N.G. Hoffman, J.A. Nelson, and R.C. Swanstrom. 2003. Turnover of env variable region 1 and 2 genotypes in subjects with late-stage human immunodeficiency virus type 1 infection. *J. Virol.* 77:6811–6822. doi:10.1128/JVI.77.12.6811-6822.2003

Kong, L., C.C. Huang, S.J. Coales, K.S. Molnar, J. Skinner, Y. Hamuro, and P.D. Kwong. 2010. Local conformational stability of HIV-1 gp120 in unliganded and CD4-bound states as defined by amide hydrogen/deuterium exchange. *J. Virol.* 84:10311–10321. doi:10.1128/JVI.00688-10

Krachmarov, C., A. Pinter, W.J. Honnen, M.K. Gorny, P.N. Nyambi, S. Zolla-Pazner, and S.C.C. Kayman. 2005. Antibodies that are cross-reactive for human immunodeficiency virus type 1 clade a and clade B v3 domains are common in patient sera from Cameroon, but their neutralization activity is usually restricted by epitope masking. *J. Virol.* 79:780–790. doi:10.1128/JVI.79.2.780-790.2005

Krachmarov, C.P., W.J. Honnen, S.C. Kayman, M.K. Gorny, S. Zolla-Pazner, and A.C. Pinter. 2006. Factors determining the breadth and potency of neutralization by V3-specific human monoclonal antibodies derived from subjects infected with clade A or clade B strains of human immunodeficiency virus type 1. *J. Virol.* 80:7127–7135. doi:10.1128/JVI.02619-05

Kwong, P.D., R. Wyatt, J. Robinson, R.W. Sweet, J. Sodroski, and W.A. Hendrickson. 1998. Structure of an HIV gp120 envelope glycoprotein in complex with the CD4 receptor and a neutralizing human antibody. *Nature.* 393:648–659. doi:10.1038/31405

Kwong, P.D., R. Wyatt, Q.J. Sattentau, J. Sodroski, and W.A. Hendrickson. 2000. Oligomeric modeling and electrostatic analysis of the gp120 envelope glycoprotein of human immunodeficiency virus. *J. Virol.* 74:1961–1972. doi:10.1128/JVI.74.4.1961-1972.2000

Kwong, P.D., M.L. Doyle, D.J. Casper, C. Cicala, S.A. Leavitt, S. Majeed, T.D. Steenbeke, M. Venturi, I. Chaiken, M. Fung, et al. 2002. HIV-1 evades antibody-mediated neutralization through conformational masking of receptor-binding sites. *Nature.* 420:678–682. doi:10.1038/nature01188

Laakso, M.M., F.H. Lee, B. Haggarty, C. Agrawal, K.M. Nolan, M. Biscone, J. Romano, A.P. Jordan, G.J. Leslie, E.G. Meissner, et al. 2007. V3 loop truncations in HIV-1 envelope impart resistance to coreceptor inhibitors and enhanced sensitivity to neutralizing antibodies. *PLoS Pathog.* 3:e117. doi:10.1371/journal.ppat.0030117

Liu, J., A. Bartesaghi, M.J. Borgnia, G. Sapiro, and S.C. Subramaniam. 2008a. Molecular architecture of native HIV-1 gp120 trimers. *Nature.* 455:109–113. doi:10.1038/nature07159

Liu, Y., M.E. Curlin, K. Diem, H. Zhao, A.K. Ghosh, H. Zhu, A.S. Woodward, J. Maenza, C.E. Stevens, J. Stekler, et al. 2008b. Env length and N-linked glycosylation following transmission of human immunodeficiency virus Type 1 subtype B viruses. *Virology.* 374:229–233. doi:10.1016/j.virol.2008.01.029

Losman, B., A. Bolmstedt, K. Schønning, Björndal A, C. Westin, E.M. Fenyö, and S. Olofsson. 2001. Protection of neutralization epitopes in the V3 loop of oligomeric human immunodeficiency virus type 1 glycoprotein 120 by N-linked oligosaccharides in the V1 region. *AIDS Res. Hum. Retroviruses.* 17:1067–1076. doi:10.1089/088922201300343753

Ly, A., and L. Stamatatos. 2000. V2 loop glycosylation of the human immunodeficiency virus type 1 SF162 envelope facilitates interaction of this protein with CD4 and CCR5 receptors and protects the virus from neutralization by anti-V3 loop and anti-CD4 binding site antibodies. *J. Virol.* 74:6769–6776. doi:10.1128/JVI.74.15.6769-6776.2000

Magnus, C., and R.R. Regoes. 2010. Estimating the stoichiometry of HIV neutralization. *PLOS Comput. Biol.* 6:e1000713. doi:10.1371/journal.pcbi.1000713

Masciotra, S., S.M. Owen, D. Rudolph, C. Yang, B. Wang, N. Saksena, T. Spira, S. Dhawan, and R.B. Lal. 2002. Temporal relationship between V1V2 variation, macrophage replication, and coreceptor adaptation during HIV-1 disease progression. *AIDS.* 16:1887–1898. doi:10.1097/00002030-200209270-00005

Moore, J.P., J.A. McKeating, R.A. Weiss, and Q.J. Sattentau. 1990. Dissociation of gp120 from HIV-1 virions induced by soluble CD4. *Science.* 250:1139–1142. doi:10.1126/science.2251501

Moore, P.L., E.T. Crooks, L. Porter, P. Zhu, C.S. Cayanan, H. Grise, P. Corcoran, M.B. Zwick, M. Franti, L. Morris, et al. 2006. Nature of nonfunctional envelope proteins on the surface of human immunodeficiency virus type 1. *J. Virol.* 80:2515–2528. doi:10.1128/JVI.80.5.2515-2528.2006

Morikita, T., Y. Maeda, S. Fujii, S. Matsushita, K. Obaru, and K. Takatsuki. 1997. The V1/V2 region of human immunodeficiency virus type 1 modulates the sensitivity to neutralization by soluble CD4 and cellular tropism. *AIDS Res. Hum. Retroviruses.* 13:1291–1299. doi:10.1089/aid.1997.13.1291

Palmer, C., P. Balfe, D. Fox, J.C. May, R. Frederiksson, E.M. Fenyö, and J.A. McKeating. 1996. Functional characterization of the V1V2 region of human immunodeficiency virus type 1. *Virology.* 220:436–449. doi:10.1006/viro.1996.0331

Pancera, M., S. Majeed, Y.E. Ban, L. Chen, C.C. Huang, L. Kong, Y.D. Kwon, J. Stuckey, T. Zhou, J.E. Robinson, et al. 2010. Structure of HIV-1 gp120 with gp41-interactive region reveals layered envelope architecture and basis of conformational mobility. *Proc. Natl. Acad. Sci. USA.* 107:1166–1171. doi:10.1073/pnas.0911004107

Pastore, C., R. Nedellec, A. Ramos, S. Pontow, L. Ratner, and D.E.C. Mosier. 2006. Human immunodeficiency virus type 1 coreceptor switching: V1/V2 gain-of-fitness mutations compensate for V3 loss-of-fitness mutations. *J. Virol.* 80:750–758. doi:10.1128/JVI.80.2.750-758.2006

Pinter, A., W.J. Honnen, Y. He, M.K. Gorny, S. Zolla-Pazner, and S.C. Kayman. 2004. The V1/V2 domain of gp120 is a global regulator of the sensitivity of primary human immunodeficiency virus type 1 isolates to neutralization by antibodies commonly induced upon infection. *J. Virol.* 78:5205–5215. doi:10.1128/JVI.78.10.5205-5215.2004

Pugach, P., S.E. Kuhmann, J. Taylor, A.J. Marozsan, A. Snyder, T. Ketas, S.M. Wolinsky, B.T. Korber, and J.P. Moore. 2004. The prolonged culture of human immunodeficiency virus type 1 in primary lymphocytes increases its sensitivity to neutralization by soluble CD4. *Virology.* 321:8–22. doi:10.1016/j.virol.2003.12.012

Rieder, P., B. Joos, V. von Wyl, H. Kuster, C. Grube, C. Leemann, J. Böni, S. Yerly, T. Klimkait, P. Bürgisser, et al; Swiss HIV Cohort Study. 2010. HIV-1 transmission after cessation of early antiretroviral therapy among men having sex with men. *AIDS.* 24:1177–1183. doi:10.1097/QAD.0b013e328338e4de

Ritola, K., C.D. Pilcher, S.A. Fiscus, N.G. Hoffman, J.A. Nelson, K.M. Kitrinos, C.B. Hicks, J.J. Eron Jr., and R.C. Swanstrom. 2004. Multiple V1/V2 env variants are frequently present during primary infection with human immunodeficiency virus type 1. *J. Virol.* 78:11208–11218. doi:10.1128/JVI.78.20.11208-11218.2004

Ruprecht, C.R., A. Krarup, L. Reynell, A.M. Mann, O.F. Brandenberg, L. Berlinger, I.A. Abela, R.R. Regoes, H.F. Günthard, P. Rusert, and A. Trkola. 2011. MPER-specific antibodies induce gp120 shedding and irreversibly neutralize HIV-1. *J. Exp. Med.* 208:439–454. doi:10.1084/jem.20101907

Rusert, P., A. Mann, M. Huber, V. von Wyl, H.F. Gunthard, and A. Trkola. 2009. Divergent effects of cell environment on HIV entry inhibitor activity. *AIDS.* 23:1319–1327. doi:10.1097/QAD.0b013e32832d92c2

Sagar, M., X. Wu, S. Lee, and J. Overbaugh. 2006. Human immunodeficiency virus type 1 V1-V2 envelope loop sequences expand and add glycosylation sites over the course of infection, and these modifications affect antibody neutralization sensitivity. *J. Virol.* 80:9586–9598. doi:10.1128/JVI.00141-06

Sanders, R.W., L. Schiffner, A. Master, F. Kajumo, Y. Guo, T. Dragic, J.P. Moore, and J.M. Binley. 2000. Variable-loop-deleted variants of the human immunodeficiency virus type 1 envelope glycoprotein can be stabilized by an intermolecular disulfide bond between the gp120 and gp41 subunits. *J. Virol.* 74:5091–5100. doi:10.1128/JVI.74.11.5091-5100.2000

Saunders, C.J., R.A. McCaffrey, I. Zharkikh, Z. Kraft, S.E. Malenbaum, B. Burke, C. Cheng-Mayer, and L. Stamatatos. 2005. The V1, V2, and V3 regions of the human immunodeficiency virus type 1 envelope differentially affect the viral phenotype in an isolate-dependent manner. *J. Virol.* 79:9069–9080. doi:10.1128/JVI.79.14.9069-9080.2005

Schoeni-Affolter, F., B. Ledergerber, M. Rickenbach, C. Rudin, H.F. Günthard, A. Telenti, H. Furrer, S. Yerly, and P. Francioli; Swiss HIV Cohort Study. 2010. Cohort profile: the Swiss HIV Cohort study. *Int. J. Epidemiol.* 39:1179–1189. doi:10.1093/ije/dyp321

Shibata, J., K. Yoshimura, A. Honda, A. Koito, T. Murakami, and S. Matsushita. 2007. Impact of V2 mutations on escape from a potent neutralizing anti-V3 monoclonal antibody during in vitro selection of a primary human immunodeficiency virus type 1 isolate. *J. Virol.* 81:3757–3768. doi:10.1128/JVI.01544-06

Shioda, T., S. Oka, X. Xin, H. Liu, R. Harukuni, A. Kurotani, M. Fukushima, M.K. Hasan, T. Shiino, Y. Takebe, et al. 1997. In vivo sequence variability of human immunodeficiency virus type 1 envelope gp120:

association of V2 extension with slow disease progression. *J. Virol.* 71:4871–4881.

Stamatatos, L., and C. Cheng-Mayer. 1998. An envelope modification that renders a primary, neutralization-resistant clade B human immunodeficiency virus type 1 isolate highly susceptible to neutralization by sera from other clades. *J. Virol.* 72:7840–7845.

Stamatatos, L., M. Wiskerchen, and C. Cheng-Mayer. 1998. Effect of major deletions in the V1 and V2 loops of a macrophage-tropic HIV type 1 isolate on viral envelope structure, cell entry, and replication. *AIDS Res. Hum. Retroviruses.* 14:1129–1139. doi:10.1089/aid.1998.14.1129

Sullivan, N., Y. Sun, Q. Sattentau, M. Thali, D. Wu, G. Denisova, J. Gershoni, J. Robinson, J. Moore, and J. Sodroski. 1998. CD4-induced conformational changes in the human immunodeficiency virus type 1 gp120 glycoprotein: consequences for virus entry and neutralization. *J. Virol.* 72:4694–4703.

Trkola, A., H. Kuster, C. Leemann, A. Oxenius, C. Fagard, H. Furrer, M. Battegay, P. Vernazza, E. Bernasconi, R. Weber, et al; Swiss HIV Cohort Study. 2004. Humoral immunity to HIV-1: kinetics of antibody responses in chronic infection reflects capacity of immune system to improve viral set point. *Blood.* 104:1784–1792. doi:10.1182/blood-2004-01-0251

Walker, L.M., S.K. Phogat, P.Y. Chan-Hui, D. Wagner, P. Phung, J.L. Goss, T. Wrin, M.D. Simek, S. Fling, J.L. Mitcham, et al; Protocol G Principal Investigators. 2009. Broad and potent neutralizing antibodies from an African donor reveal a new HIV-1 vaccine target. *Science.* 326:285–289. doi:10.1126/science.1178746

White, T.A., A. Bartesaghi, M.J. Borgnia, J.R. Meyerson, M.J. de la Cruz, J.W. Bess, R. Nandwani, J.A. Hoxie, J.D. Lifson, J.L. Milne, and S. Subramaniam. 2010. Molecular architectures of trimeric SIV and HIV-1 envelope glycoproteins on intact viruses: strain-dependent variation in quaternary structure. *PLoS Pathog.* 6:e1001249. doi:10.1371/journal.ppat.1001249

Wu, S.R., R. Löving, B. Lindqvist, H. Hebert, P.J. Koeck, M. Sjöberg, and H. Garoff. 2010. Single-particle cryoelectron microscopy analysis reveals the HIV-1 spike as a tripod structure. *Proc. Natl. Acad. Sci. USA.* 107:18844–18849. doi:10.1073/pnas.1007227107

Wyatt, R., N. Sullivan, M. Thali, H. Repke, D. Ho, J. Robinson, M. Posner, and J. Sodroski. 1993. Functional and immunologic characterization of human immunodeficiency virus type 1 envelope glycoproteins containing deletions of the major variable regions. *J. Virol.* 67:4557–4565.

Wyatt, R., J. Moore, M. Accola, E. Desjardin, J. Robinson, and J. Sodroski. 1995. Involvement of the V1/V2 variable loop structure in the exposure of human immunodeficiency virus type 1 gp120 epitopes induced by receptor binding. *J. Virol.* 69:5723–5733.

Xiang, S.H., A. Finzi, B. Pacheco, K. Alexander, W. Yuan, C. Rizzuto, C.C. Huang, P.D. Kwong, and J.C. Sodroski. 2010. A V3 loop-dependent gp120 element disrupted by CD4 binding stabilizes the human immunodeficiency virus envelope glycoprotein trimer. *J. Virol.* 84:3147–3161. doi:10.1128/JVI.02587-09

Zanetti, G., J.A. Briggs, K. Grünewald, Q.J. Sattentau, and S.D. Fuller. 2006. Cryo-electron tomographic structure of an immunodeficiency virus envelope complex in situ. *PLoS Pathog.* 2:e83. doi:10.1371/journal.ppat.0020083

Zhou, T., L. Xu, B. Dey, A.J. Hessell, D. Van Ryk, S.H. Xiang, X. Yang, M.Y. Zhang, M.B. Zwick, J. Arthos, et al. 2007. Structural definition of a conserved neutralization epitope on HIV-1 gp120. *Nature.* 445:732–737. doi:10.1038/nature05580

Zhu, P., J. Liu, J. Bess Jr., E. Chertova, J.D. Lifson, H. Grisé, G.A. Ofek, K.A. Taylor, and K.H. Roux. 2006. Distribution and three-dimensional structure of AIDS virus envelope spikes. *Nature.* 441:847–852. doi:10.1038/nature04817